

This discussion paper is/has been under review for the journal Hydrology and Earth System Sciences (HESS). Please refer to the corresponding final paper in HESS if available.

Estimating annual effective infiltration coefficient and groundwater recharge for karst aquifers of the southern Apennines

V. Allocca, F. Manna, and P. De Vita

Dipartimento di Scienze della Terra, dell'Ambiente e delle Risorse – University of Naples “Federico II”, Italy

Received: 24 July 2013 – Accepted: 27 July 2013 – Published: 7 August 2013

Correspondence to: V. Allocca (vincenzo.allocca@unina.it)

Published by Copernicus Publications on behalf of the European Geosciences Union.

HESSD

10, 10127–10159, 2013

Estimating annual effective infiltration coefficient

V. Allocca et al.

Title Page	
Abstract	Introduction
Conclusions	References
Tables	Figures
◀	▶
◀	▶
Back	Close
Full Screen / Esc	
Printer-friendly Version	
Interactive Discussion	

Abstract

To assess the mean annual groundwater recharge of the karst aquifers in southern Apennines (Italy), the estimation of the mean annual effective infiltration coefficient (AEIC) was conducted by means of an integrated approach based on hydrogeological, 5 hydrological, geomorphological, land use and soil cover analyses. We studied a large part of the southern Apennines that is covered by a meteorological network and containing 40 principal karst aquifers. Using precipitation and air temperature time series gathered through monitoring stations operating in the period 1926–2012, the annual 10 effective precipitation (AEP) was estimated, and its distribution was modelled, by considering the orographic barrier and rain shadow effects of the Apennines chain, as well as the altitudinal control. Four sample karst aquifers with available long spring 15 discharge time series were identified for estimating the AEIC by means of the hydrological budget equation. The resulting AEIC values were correlated with other parameters that control groundwater recharge, such as the extension of outcropping karst-rock, morphological settings, land use and covering soil type. A simple correlation relationship 20 between AEIC, lithology and the summit flat and endorheic areas was found. This empirical model has been used to estimate AEIC and mean annual groundwater recharge in other regional karst aquifers. The estimated AEIC values ranged between 48 % and 78 %, thus matching intervals estimated for other karst aquifers in European and Mediterranean countries.

These results represent a deeper understanding of an aspect of groundwater hydrology in karst aquifers which is fundamental for the formulation of appropriate management models of groundwater resources, also taking into account mitigation strategies for climate change impacts. Finally, the proposed hydrological characterisations 25 are also perceived as useful for the assessment of mean annual runoff over carbonate mountains, which is another important topic concerning water management in the southern Apennines.

1 Introduction

Karst aquifers host important groundwater resources for human and agricultural use in many areas of the world and include natural landscapes and ecosystems with great geo- and biodiversities (Goldscheider, 2012). For regions in southern Italy,

5 these aquifers are the primary source of drinking water and a strategic resource for socio-economic and environmental development (Allocca et al., 2007); moreover their groundwater resources play a primary role in regulating the hydro-ecological regime of rivers. In this area, the public water supplies of major cities, such as Naples, which has approximately 1.0 million inhabitants, and many small towns and countless settlements
10 are fed by large and small karst springs. Karst groundwater resources have also been utilised since the Roman epoch for drinking water (for example Augustan Aqueduct, dated 33–12 BC) and thermal and mineral water. These aquifers are currently important sources also for several bottling plants. Hence, the correct estimation at various
15 space-time scales of groundwater recharge processes in karst systems, taking into account atmospheric decadal variability (De Vita et al., 2012a), is a fundamental and challenging issue to be investigated to properly manage groundwater as well as surface resources with respect to the EU Water Framework Directive (European Commission, 2000).

20 A wide range of direct and indirect approaches to estimate groundwater recharge processes, with the degree of approximation depending on different space-time scales, have been proposed (Scanlon et al., 2002 and references therein). Examples include lysimeter measurements, soil moisture budgets and effective infiltration coefficients, as well as water table rise, tracer and remote sensing methods. At a regional scale, groundwater recharge can be assessed by multi-disciplinary analyses of hydrological
25 time series plus hydrogeological and geomorphological data in a GIS environment to estimate the endogenous and exogenous variables affecting the recharge processes (Andreo et al., 2008; Dripps and Bradbury, 2010).

Estimating annual effective infiltration coefficient

V. Allocca et al.

[Title Page](#)

[Abstract](#)

[Introduction](#)

[Conclusions](#)

[References](#)

[Tables](#)

[Figures](#)

[◀](#)

[▶](#)

[◀](#)

[▶](#)

[Back](#)

[Close](#)

[Full Screen / Esc](#)

[Printer-friendly Version](#)

[Interactive Discussion](#)



Estimating annual effective infiltration coefficient

V. Allocata et al.

[Title Page](#)[Abstract](#)[Introduction](#)[Conclusions](#)[References](#)[Tables](#)[Figures](#)[|◀](#)[▶|](#)[◀](#)[▶](#)[Close](#)[Full Screen / Esc](#)[Printer-friendly Version](#)[Interactive Discussion](#)

The paper is organised as follows: after a description of the issue and a review of the literature in Sect. 1, we present the hydrogeological characteristics of the karst aquifers of the southern Apennines in Sect. 2 followed by the data and methods, results, discussion and concluding remarks in Sects. 3, 4 and 5, respectively.

5 2 Hydrogeology of karst aquifers and climatic characteristics of the southern Apennines

The southern Apennines consist of a series of mountain ranges in which karst aquifers form the major massifs (Fig. 1). In this area, karst aquifers cover approximately 8560 km² (Fig. 1) and consist mainly of Triassic–Liassic dolomites, Jurassic limestones and Paleogene marly limestones of the Mesozoic carbonate platform series, which were tectonically deformed and piled up in the fold-and-thrust belt Apennines structure during the Miocene orogenic phases (Patacca and Scandone, 2007). The karst aquifers of the southern Apennines in several cases are characterised by large flat surface and endorheic zones on the top and exhibit an average inclination of structurally controlled slopes of approximately 30°–35°, related to the morphological evolution of original fault line scarps (Brancaccio et al., 1978; Bull, 2007). Moreover, given their proximity to volcanic centres (Fig. 1), these aquifers were singularly covered by variable thicknesses of ash-fall pyroclastic deposits (De Vita et al., 2006, 2012b) that erupted during the Quaternary, whose presence influences epikarst development (Celico et al., 2010).

20 According to conceptual models of groundwater circulation in karst aquifers (White, 1969, 2002; Mangin, 1975a, b, c; Kiraly, 1975, 2002; Drouge, 1992; Bonacci, 1993; Klimchouk, 2000; Civita et al., 1992; Goldscheider and Drew, 2007; Fiorillo, 2011), those of the southern Apennines host huge groundwater bodies outflowing chiefly in basal springs with mean annual discharges varying from 0.1 to 5.5 m³ s⁻¹. Due to the 25 fold-and-thrust belt structure of the Apennine, karst aquifers are tectonically juxtaposed to hydrostratigraphic units of lower permeability belonging to pre- and syn-orogenic basinal and flysch series. Therefore, the groundwater circulation of karst aquifers is

Estimating annual effective infiltration coefficient

V. Allocata et al.

[Title Page](#)

[Abstract](#)

[Introduction](#)

[Conclusions](#)

[References](#)

[Tables](#)

[Figures](#)

[◀](#)

[▶](#)

[◀](#)

[▶](#)

[Back](#)

[Close](#)

[Full Screen / Esc](#)

[Printer-friendly Version](#)

[Interactive Discussion](#)



basically controlled by the geometry of stratigraphic or tectonic contacts with these units of lower permeability, being generally oriented toward the lowest point of the hydrogeological boundary (Celico, 1983; Allocca et al., 2007), where basal springs are located (Fig. 1). In these zones, the groundwater circulation can also feed alluvial and detrital aquifers in lateral contact with karst aquifers. Other minor stratigraphic or tectonic factors subdivide the basal groundwater circulation inside karst aquifers. These include faults with low-permeability damage zones or intervals in the carbonate series with marly or argillaceous composition that compartmentalise the aquifers in basin-in-series systems (Celico, 1983; Celico et al., 2006).

A subordinate perched groundwater flow also occurs in the surficial part of karst aquifers, where stratigraphic and structural factors or the presence of small karst conduits can generate high-altitude seasonal and ephemeral springs characterised by mean annual discharges generally lower than $0.01 \text{ m}^3 \text{ s}^{-1}$. The groundwater recharge of karst aquifers occurs by diffuse-direct net infiltration through the epikarst (autogenic recharge) and concentrated-secondary infiltration of runoff formed on the surrounding or overlying non-karst terrains (allogenic recharge). For several karst aquifers of the southern Apennines, the mean annual groundwater flow was assessed mostly on the basis of short-duration time series or few measurements of spring discharges.

The climatic characteristics of the southern Apennines and their temporal variability strongly control the recharge processes in karst aquifers, and both are controlled by the North Atlantic Oscillation (De Vita et al., 2012a). The climate of this sector of Italy varies from Mediterranean type (Csa) in the coastal sector to Mediterranean mild climate (CSb) in the inland areas (Geiger, 1954). The spatial distribution of mean annual precipitation is chiefly influenced by the orographic effect (Henderson-Sellers and Robinson, 1986) of the Apennine mountain ranges on humid air masses moving eastward from the Tyrrhenian Sea. According to the location of the Apennine chain, higher orographic precipitation occurs in the western sector, with maximum values up to 1700–2000 mm along the Apennines ridge itself. Eastward of the Apennines ridge,

Estimating annual effective infiltration coefficient

V. Allocca et al.

[Title Page](#)

[Abstract](#)

[Introduction](#)

[Conclusions](#)

[References](#)

[Tables](#)

[Figures](#)

[◀](#)

[▶](#)

[◀](#)

[▶](#)

[Back](#)

[Close](#)

[Full Screen / Esc](#)

[Printer-friendly Version](#)

[Interactive Discussion](#)



lower precipitations down to 700–900 mm are recorded because of the rain shadow effect.

3 Data and methods

Analyses were carried out in a large sector of the southern Apennines covering approximately 19 339 km², corresponding to the regional hydrological network of the National Hydrographic and Tidal Service, Department of Naples. We assessed the basic hydrogeological characteristics that control groundwater recharge in karst aquifers over this territory (Fig. 1): aquifer extension, outcropping lithology, morphological settings (slope angle distribution and summit flat/endorheic areas), land use and type of soil cover. We also collected and analysed the precipitation and air temperature time series recorded by all monitoring stations functioning over the same territory in the period 1926–2012. Moreover, four sample karst aquifers were identified to estimate the AEIC on the basis of the availability of significant spring discharge time series and representativeness of the lithological and morphological settings (Fig. 1): the Matese (a), Accellica (a), Terminio and Cervialto karst aquifers. Although not numerous, the examined sample aquifers are the only ones for which long time series of spring discharges are available in the southern Apennines.

3.1 Aquifer lithology, covering soil type, land use and geomorphological data

On the basis of preceding hydrogeological studies carried out for singular aquifers and synthesised in reviews of regional relevance (Celico, 1983; Allocata et al., 2009), 20 40 principal karst aquifers were identified (Fig. 1). The outcropping lithology of the karst aquifers were assessed by analysing hydrogeological maps of southern Italy, 1 : 250 000 scale (Allocata et al., 2007).

To analyse the types of soil covering such aquifers, the Land System Map of the 25 Campania Region, 1 : 250 000 scale (www.risorsa.info), and the Ecopedological Map of

[Title Page](#)

[Abstract](#)

[Introduction](#)

[Conclusions](#)

[References](#)

[Tables](#)

[Figures](#)

[◀](#)

[▶](#)

[◀](#)

[▶](#)

[Back](#)

[Close](#)

[Full Screen / Esc](#)

[Printer-friendly Version](#)

[Interactive Discussion](#)



Italy, 1 : 250 000 scale (www.pcn.minambiente.it), were consulted and data from Corine Land Cover 2006 (www.eea.europa.eu) were collected to analyse land use. A 20 m grid spacing digital elevation model was **constructed** to examine the morphological features of the karst aquifers, giving special attention to slope angle and **extension**

5 **of the endorheic watersheds**. The above-mentioned spatial data were implemented in a geographical information system, which allowed us to analyse **the spatial frequency** of such parameters for each examined **karst aquifer**.

3.2 Hydrological data

The mean annual precipitation data (387 rain gauge stations) and air temperatures (228 monitoring stations) were gathered from the annals of the National Hydrographic and Tidal Service in the period 1926–1999 (www.isprambiente.gov.it) and Regional Civil Protection Agency databases (www.protezionecivile.gov.it) for the remaining interval from 2000 to 2012. During the entire period, the number of rain gauge stations varied from a total of 175 in 1926 to a minimum of 52 during 1943–1944, up to a maximum of 225 from 1972 to 1984 to a current value of 171. The number of the air temperature stations began with 19 in 1926, increased to 90 in 1975, and then oscillated around this number up to now. Nevertheless, more than 50 % of the monitoring stations worked for longer than 30 yr and approximately 10 % of the stations ran for more than 70 yr. Another issue of this monitoring network was the prevailing distribution of 15 stations in the lower-middle altitude ranges (0–600 m a.s.l.), which is a limiting factor in 20 assessing hydrological data at the highest altitude ranges.

25 Time series were analysed to reconstruct regional distribution models of mean annual precipitation, air temperature and effective precipitation, thereby accounting for variations due to orographic control of mountain ranges (Roe, 2005; Houze, 2012) and altitude (Vuglinski, 1972; Brunsdon et al., 2001) in a GIS environment. For the effective precipitation data set, a linear correlation analysis between mean annual values and altitude of each station was carried out identifying subzones with a homogeneous relationship **between effective precipitation and altitude**. For each effective precipitation

[Title Page](#)

[Abstract](#)

[Introduction](#)

[Conclusions](#)

[References](#)

[Tables](#)

[Figures](#)

[◀](#)

[▶](#)

[◀](#)

[▶](#)

[Back](#)

[Close](#)

[Full Screen / Esc](#)

[Printer-friendly Version](#)

[Interactive Discussion](#)



zone, an empirical model was calculated by means of a linear regression weighted by the number of years of functioning of each station (Carroll and Ruppert, 1988).

To estimate the mean annual effective precipitation over the period 1926–2012, the actual evapotranspiration was calculated for each rain gauge station by Turc's formula (Turc, 1954), the reliability of which was confirmed by other studies in the Mediterranean area (Santoro, 1970; Boni et al., 1982):

$$ETR_j = \frac{AP_j}{\sqrt{0.9 + \left(\frac{AP_j}{300 + 25 \cdot AT_j + 0.05 \cdot AT_j^3} \right)^2}} \quad (1)$$

where ETR_j is the mean annual actual evapotranspiration (mm) for the j rain gauge station; AP_j is the mean annual precipitation (mm) for the j rain gauge station; and AT_j is the mean annual air temperature ($^{\circ}$ C) for the j air temperature-rain gauge station.

The actual evapotranspiration was also calculated for those rain gauge stations not provided with an air temperature sensor. In this case, the mean air annual temperature (AT_j) was estimated by the empirical (linear regression model with the altitude, which was found to be unique at the regional scale and statistically robust.

Finally, the mean annual effective precipitation (AEP_j) for the j rain gauge station was calculated by

$$AEP_j = AP_j - ETR_j \quad (2)$$

To estimate the mean annual spring discharges, the discharge time series of basal springs of the sample karst aquifers were analysed (Fig. 1). Specifically for the Matese

(a) karst aquifer, the Maretto and Torano springs were considered (recording period from 1967–2000 and 1957–2000, respectively). For the Terminio aquifer, we analysed the Cassano Irpino (recording period 1965–2010), Serino (recording period 1887–2010) and Baiardo and Salza Irpina springs (recording period 1970–2000). For the Cervialto aquifer, the Sanità spring, which represents the sole outflow of the entire

Estimating annual effective infiltration coefficient

V. Allocata et al.

[Title Page](#)

[Abstract](#)

[Introduction](#)

[Conclusions](#)

[References](#)

[Tables](#)

[Figures](#)

[◀](#)

[▶](#)

[◀](#)

[▶](#)

[Back](#)

[Close](#)

[Full Screen / Esc](#)

[Printer-friendly Version](#)

[Interactive Discussion](#)



karst aquifer and a unique case for the duration of its time series (recording period 1921–2012), was considered (De Vita et al., 2012a). For the Accellica (a) karst aquifer, we analysed the Avella and Ausino–Ausinetto springs (recording period 1967–1989).

3.3 Hydrological budget of karst aquifers and AEIC estimation

5 The AEIC was estimated for each of the four sample karst aquifers, by applying the hydrological budget equation to mean the values for the period 1926–2012:

$$AP + U_i = ETR + R + IE + U_u + Q_s + Q_t \pm \Delta W_r \quad (3)$$

where AP is the mean annual precipitation, U_i is the mean annual indirect inflow discharge, ETR is the mean annual actual evapotranspiration, R is the mean annual runoff, IE is the mean annual direct net infiltration, U_u is the mean annual indirect outflow discharge, Q_s is the mean annual spring discharges, Q_t is the mean annual tapped discharge and $\pm \Delta W_r$ is the interannual variation of groundwater reserves.

Because interannual variations of groundwater reserves ($\pm \Delta W_r$) are negligible in the long-term, Eq. (1) can be simplified as follows:

$$15 AP + U_i = ETR + R + IE + U_u + Q_s + Q_t \quad (4)$$

Groundwater inflows (U_i) and losses (U_u) through juxtaposed alluvial and detrital aquifers were estimated by the application of Darcy's law (Darcy, 1856) to the hydrogeological parameters of the adjoining aquifers.

The mean AEIC was estimated for each karst aquifer as the ratio between the mean annual outflow ($V_{\text{outflow}} = U_u + Q_s + Q_p$) and the annual mean inflow ($V_{\text{inflow}} = AP - ETR + U_i$), where both were related to the whole extension of the aquifer:

$$AEIC = \left[\frac{U_u + Q_s + Q_p}{AP - ETR + U_i} \right] \times 100 \quad (5)$$

[Title Page](#)

[Abstract](#)

[Introduction](#)

[Conclusions](#)

[References](#)

[Tables](#)

[Figures](#)

◀

▶

◀

▶

[Back](#)

[Close](#)

[Full Screen / Esc](#)

[Printer-friendly Version](#)

[Interactive Discussion](#)



Furthermore, due to the peculiar morphological setting of karst aquifers, summit flat areas (slope angle $\leq 5^\circ$) and endorheic watersheds, in which the infiltration value reaches the maximum value (AEIC = 100 %), were identified and measured (Fig. 3d). The annual effective infiltration coefficient for the slope part (AEIC_S), in non-endorheic conditions and with slope angle greater than 5°, was therefore calculated by the following formula:

$$\text{AEIC}_S = \left[\frac{(\text{AEIC} \times A_T) - (1 \times A_E)}{A_T - A_E} \right] \times 100 \quad (6)$$

where A_T is the total area of the karst aquifer (km^2), and A_E is the cumulative extension of summit flat areas and/or endorheic watersheds (km^2).

This estimation was considered useful for a comprehensive understanding of the hydrological role of karst aquifers, and thus also for taking into account a general assessment of runoff formation along karst slopes (Horvat and Rubinic, 2006) by estimating the annual runoff coefficient (ARC), which is the complementary part of the AEIC ($\text{ARC} = 100 - \text{AEIC}_S$).

To test the sensitivity of the AEIC estimation due to the annual variability of inflow and outflow volumes, minimum and maximum values of the AEIC and AEIC_S were estimated by considering the 95 % confidence limits of the effective precipitation and air temperature empirical models.

4 Results

4.1 Aquifer extensions and lithology

Aquifer extensions and the lithology of the 40 karst aquifers were assessed by analysing regional hydrogeological maps (Allocacca et al., 2007). Specifically, the four sample karst aquifers were shown to be representative, both by their significant extensions and their outcropping lithology (Fig. 2d): Matese (a) (120 km^2 ; 97 % limestone

Estimating annual effective infiltration coefficient

V. Allocacca et al.

[Title Page](#)

[Abstract](#)

[Introduction](#)

[Conclusions](#)

[References](#)

[Tables](#)

[Figures](#)

[◀](#)

[▶](#)

[◀](#)

[▶](#)

[Back](#)

[Close](#)

[Full Screen / Esc](#)

[Printer-friendly Version](#)

[Interactive Discussion](#)



and 3 % dolomite); Accellica (a) (35 km^2 ; 68 % dolomite and 32 % limestone); Terminio (167 km^2 ; 100 % limestone) and Cervialto (129 km^2 ; 98 % limestone and 2 % dolomite).

4.2 Soil type, land use and geomorphological features

Our analysis of the soil types covering karst aquifers identified the loamy sand type (coded as LS in Fig. 2a) as the prevailing one with a percentage greater than 90 % for three of the four karst aquifers considered, which is consistent with Naclerio et al. (2008) and Naclerio et al. (2009). A fraction of a coarser soil type, 14 % of sandy loam soils (coded as SL in Fig. 2a), was identified for the Terminio karst aquifer according to other studies carried out at a detailed scale (Allocca et al., 2008) and the proximity to the Somma–Vesuvius volcano, which led to the deposition both of greater thicknesses of ash-fall pyroclastic deposits (De Vita et. al., 2006) and coarser grain sizes.

Land use varied among four principal typologies: woodland, meadowland, areas without vegetation cover and urban areas. Specifically, the woodland and meadow-land classes were the dominant ones in the four sample karst aquifers, extending for approximately 85 % and 14 % of the total area, respectively (Fig. 2b).

We found the sample karst aquifers to have extensions of summit flat areas and endorheic zones (Fig. 2d) varying from 43 % in the case of Terminio to 0 % Accellica (a), with intermediate values of approximately 35 % and 20 % for Matese (a) and Cervialto, respectively. Moreover, the cumulative distributions of slope angle were found to be similar across the sample (Fig. 2c) and other aquifers (Fig. 3c), showing a similar median value of 25° .

Considering the 40 karst aquifers identified at a regional scale (Fig. 1), the soil type was notably homogeneous (Fig. 3a) with a prevalence of sand in each category. We found average land use values of 69 % for woodland, 25 % for meadowland, 5 % for areas without vegetation and 1 % for urban areas (Fig. 3b). The morphological settings of all karst aquifers showed very similar cumulative distributions of slope angles,

[Title Page](#)

[Abstract](#)

[Introduction](#)

[Conclusions](#)

[References](#)

[Tables](#)

[Figures](#)

[◀](#)

[▶](#)

[◀](#)

[▶](#)

[Back](#)

[Close](#)

[Full Screen / Esc](#)

[Printer-friendly Version](#)

[Interactive Discussion](#)



with a median of 25° and a modal value ranging within 20°–25°. In contrast, the most frequent higher value slope angle class was 30°–35°, according to the typical morphological setting due to the erosional evolution of fault-line scarps in carbonate mountains of the southern Apennines (Brancaccio et al., 1978; Bull, 2007). Significant differences 5 were observed in the distribution and extent of the summit flat and endorheic areas (Fig. 3d and Table 2) according to the different structural settings of the karst aquifers. More extended summit flat and endorheic watersheds were detected in the northern and in the southern parts of the study area. In particular, more than 40 % of the total area of the Terminio and Alburni karst aquifers (Fig. 3d and Table 2) were characterised 10 by summit flat area and endorheic watersheds, and hence by a total effective infiltration.

4.3 Effective precipitation estimation

Despite the apparent homogeneous distribution of rain gauges and air temperature stations over the territory (Fig. 4a and b), the assessment of the spatial distribution of these stations revealed an inhomogeneous scattering with altitude, with a dominant 15 presence in the lower-middle ranges (Fig. 4c and d). This scarcity of a monitoring network at higher altitude ranges was recognised as a principal issue to overcome to assess the groundwater recharge of karst aquifers, which have a mountainous morphology extending up to the highest altitudes. In fact, the statistical comparison between the altitude of the monitoring stations and the karst aquifers showed that 50 % 20 of these areas lie at altitudes between 800 and 2280 m a.s.l., where only 10 % of rain gauge and air temperature stations are located (Fig. 4c and d).

Therefore, to estimate groundwater recharge at a regional scale, a distributed model of AEP was reconstructed by considering the spatial variability due to both orographic and altitudinal controls. By analysing the correlation of AEP data with the altitudes 25 of the rain gauge stations, we found three homogeneous effective precipitation zones according to the orographic barrier effect (Vuglinski, 1972; Brunsdon et al., 2001) of the Apennine chain. An upwind zone, extending from the coastline to the principal Apennine morphological divide, and two downwind zones eastward of the same divide

Estimating annual effective infiltration coefficient

V. Allocata et al.

[Title Page](#)

[Abstract](#)

[Introduction](#)

[Conclusions](#)

[References](#)

[Tables](#)

[Figures](#)

[◀](#)

[▶](#)

[◀](#)

[▶](#)

[Back](#)

[Close](#)

[Full Screen / Esc](#)

[Printer-friendly Version](#)

[Interactive Discussion](#)



were identified (Figs. 5 and 6), which resulted from a rain shadowing effect (Roe, 2005). For each zone, a specific linear regression model, weighted by the years of functioning of each rain gauge station was identified between AEP and altitude (Fig. 5a, b, and c). These models showed that the AEP values progressively increase with altitude even considering three different empirical laws across the Apennine chain, which were always statistically significant ($r_{\min} = 0.714$ and Prob. t Student_{max} < 0.1 %). According to the dominant control of the altitude, only one linear regression model was found between air temperature and altitude (Fig. 5d) which was statistically significant ($r = -0.856$ and Prob. t Student < 0.1 %).

On the basis of such findings, a distributed model of mean annual effective precipitations (AEP) was reconstructed by integrating the three effective precipitation zones in a GIS layer (Fig. 6). For the upwind effective pluviometric zone, the recorded values of mean annual effective precipitation ranged between 373 mm and 1606 mm, but varied from 200 to 1010 mm for the two downwind zones.

4.4 AEIC and AEIC_S estimations

From the estimation of the variables forming Eqs. (5) and (6), the AEIC and AEIC_S were estimated for the four sample karst aquifers (Table 1), which also took into account the uncertainties due to the linear regression models (95 % confidence limits) of annual effective precipitation and altitude (Fig. 7). Considering the results related to the mean value of the regression models, similar values of the AEIC were found for the Terminio, Cervialto and Matese (a) karst aquifers, corresponding to 79 %, 71 % and 69 %, respectively, whereas a value of 50 % was calculated for the Accellica (a) karst aquifer. This difference appeared to be mainly correlated to the different lithology, which is prevailingly dolomitic, and the lack of summit flat and endorheic areas for the latter case. Corresponding AEIC_S and ARC values (Table 1 and Fig. 7) were estimated as ranging from 50 % to 64 % and from 50 % to 36 %, respectively.

4.5 Assessment of groundwater recharge

To generalise the results obtained for the four sample karst aquifers, a correlation analysis was carried out among the estimated parameters: AEIC, limestone area, summit flat and endorheic area, woodland area, loamy sand soil type area and mean slope angle. Due to the similarity of their values, both for the four sample karst aquifers and the other ones (Figs. 2 and 3), the correlation analysis revealed a negligible role of the last three parameters on AEIC variability. Consequently, we found a multiple linear regression to empirically correlate the mean AEIC to the basic controlling variables, namely limestone area ($L\%$) and summit flat and endorheic area ($E\%$):

10
$$\text{AEIC} = 47.99 + 0.08L + 0.51E \quad (7)$$

which was statistically significant ($r = 0.984$; Prob. F Fisher = 3.0 %; Standard errors of 5.92, 0.06 and 0.07 for the intercept, first and second coefficient, respectively).

The preceding equation confirms the insight that the flat and endorheic area is a factor affecting the mean AEIC more strongly than lithology (outcrop of karst rocks).

15 We estimated the AEIC and AEICs values for the 40 regional karst aquifers by applying the empirical Eqs. (6) and (7) (Table 2). The minimum estimated AEIC value was calculated for the Circeo karst aquifer (48 %); the maximum value was found for the Terminio karst aquifer (78 %), with a residual of 1 % respect to that directly calculated (Table 1) and a mean global value of 59 %.

20 The estimation of the AEIC and the AEP values for each karst aquifer allowed the assessment of the respective mean annual groundwater recharge (Table 2). To validate this empirical estimation, the recharge value calculated by Eq. (7) for the four sample karst aquifers was compared with the outflow discharges. The resulting residuals between the predicted recharge and measured outflow was considered to be negligible,

25 ranging between 0 % and 10 %, and thus supporting the reliability of the empirical estimations. Moreover, the correlation between the estimated mean annual groundwater recharge and outflow assessed for 18 of the 40 karst aquifers on the basis of non-systematic spring discharges measurements, which were carried out during the 70's

[Title Page](#)

[Abstract](#)

[Introduction](#)

[Conclusions](#)

[References](#)

[Tables](#)

[Figures](#)

[◀](#)

[▶](#)

[◀](#)

[▶](#)

[Back](#)

[Close](#)

[Full Screen / Esc](#)

[Printer-friendly Version](#)

[Interactive Discussion](#)



and 80's (Celico, 1983; Allocca et al., 2007), showed a consistent value both in terms of angular and correlation coefficients (Fig. 8).

5 Discussion and conclusions

To assess mean annual groundwater recharge in karst aquifers of the southern Apennines, our approach focused on the estimation of the AEIC as a practical tool, which was already established for **karst aquifers in other countries**.

The applied methods were oriented to account for the lack of temporal and spatial hydrological time series, namely the availability of significant spring discharge measurements and effective precipitation in the high altitude ranges. Consequently, the results are based on all existing hydrological data.

A contribution to reconstruct a regional distributed model of effective precipitation that also accounts for orographic barrier and altitude controls of the Apennine chain is provided by identifying three homogeneous zones in which singular empirical laws exist relative to altitude. This approach is proposed as a simpler and more direct method for assessing distributedly effective precipitation, which is not based on geostatistical analyses of rainfall (Goovaerts, 2000; Marquinez et al., 2003) but on the recognition of the orographic barrier and altitude controls (Vuglinski, 1972; Brunsdon et al., 2001).

By applying the hydrological budget equation to effective precipitation and spring discharge data, the estimations of the AEIC for four sample karst aquifers varied from 50 % to 79 % with a mean value of 67 % and are comparable with those in the European and peri-Mediterranean areas (Burdon, 1965; Vilimonovic, 1965; **Drouge**, 1971; Bonacci, 2001). Because of the more accurate assessment of mean annual groundwater outflow and inflow volumes for the four sample karst aquifers, as well as for the duration of time series, the calculated values advance our knowledge regarding the AEIC of karst aquifers in the southern Apennines.

Using a correlation analysis of other factors recognisable as affecting groundwater recharge in sample karst aquifers, such as lithology, morphological settings, land use

[Title Page](#)

[Abstract](#)

[Introduction](#)

[Conclusions](#)

[References](#)

[Tables](#)

[Figures](#)

[|◀](#)

[▶|](#)

[◀](#)

[▶](#)

[Back](#)

[Close](#)

[Full Screen / Esc](#)

[Printer-friendly Version](#)

[Interactive Discussion](#)



and covering soil type, we found a significant empirical relationship between AEIC, lithology and summit flat and/or endorheic areas. Owing to the similarity of the other karst aquifers identified in the regional study area, an empirical estimate of the mean AEIC was also proposed for those aquifers. We therefore present a method to assess 5 groundwater recharge of karst aquifers at a regional scale.

The proposed approach highlights another complementary aspect related to the annual runoff estimation of the slope areas, which is particularly relevant for the management of surficial water resources and furnishes values of mean ARC varying from 36 % to 50 %, matching those estimations carried out for Dinaric karst aquifers (Horvat 10 and Rubinic, 2006) and some river basins of the southern continental Italy (Del Giudice et al., 2012).

The methodology is presented as a reliable system for modelling the groundwater recharge of karst aquifers at regional and mean annual scales in the case of a large territory with discontinuous and absent hydrological monitoring. It can be conceived as 15 a deeper understanding of groundwater hydrology in karst aquifers and a first step to overcome the lack of spring discharges and piezometric levels time series. The application of this method would thus permit the design of appropriate management models for groundwater and surface resources of karst aquifers as well as the setting up of accurate strategies to mitigate the effects of climate change. This achievement would 20 allow balancing environmental needs and the societal impacts of water uses, as required by the EU Water Framework Directive (European Commission, 2000).

Acknowledgements. This study was supported in part by MIUR (Research Programme PRIN 2010–2011). The authors thank Gerardo Ventafridda of the Apulian Aqueduct (www.aqp.it), who 25 provided discharge data for the Cassano Irpino and the Sanità karst springs. We also gratefully acknowledge the Department of Civil Protection of the Campania region (www.regione.campania.it), which kindly provided the rainfall and temperature data.

Estimating annual effective infiltration coefficient

V. Allocata et al.

[Title Page](#)

[Abstract](#)

[Introduction](#)

[Conclusions](#)

[References](#)

[Tables](#)

[Figures](#)

[|◀](#)

[▶|](#)

[◀](#)

[▶](#)

[Back](#)

[Close](#)

[Full Screen / Esc](#)

[Printer-friendly Version](#)

[Interactive Discussion](#)



Allocca, V., Celico, F., Celico, P., De Vita, P., Fabbrocino, S., Mattia, S., Monacelli, G., Musilli, I., Piscopo, V., Scalise, A. R., Summa, G., and Trantafoglia, G.: Illustrative Notes of the Hydrogeological Map of Southern Italy, Istituto Poligrafico e Zecca dello Stato, ISBN 88-448-0215-5, 1–211, 2007a.

Allocca, V., De Vita, P., Fabbrocino, S., and Celico, P.: The karst aquifers of the southern Apennines (Italy): a strategic groundwater resource, *Mem. Ist. It. Speleo*, II, XIX, 65–72, 2007b.

Allocca, V., Celico, F., Petrella, E., Marzullo, G., and Naclerio, G.: The role of land use and environmental factors on microbial pollution of mountainous limestone aquifers, *Environ. Geol.*, 55, 277–283, 2008.

Allocca, V., Celico, F., Celico, P., De Vita, P., Fabbrocino, S., Mattia, C., Monacelli, G., Musilli, I., Piscopo, V., Scalise, A. R., Summa, G., and Trantafoglia, G.: La carta idrogeologica dell'Italia meridionale, Metodi ed analisi territoriali per l'identificazione e la caratterizzazione dei corpi idrici sotterranei (Direttiva 2000/60/CE), L'ACQUA, 4, 21–32, 2009.

Andreو, B., Vías, J., Durán, J. J., Jiménez, P., López-Geta, J. A., and Carrasco, F.: Methodology for groundwater recharge assessment in carbonate aquifers: application to pilot sites in southern Spain, *Hydrogeol. J.*, 16, 911–925, 2008.

Bonacci, O.: Karst spring hydrographs as indicators of karst aquifers, *Hydrolog. Sci. J.*, 38, 51–62, 1993.

Bonacci, O.: Monthly and annual effective infiltration coefficients in Dinaric karst: example of the Gradole karst spring catchment, *Hydrolog. Sci. J.*, 46, 287–299, doi:10.1080/02626660109492822, 2001.

Boni, C., Bono, P., and Capelli, G.: Valutazione quantitativa dell'infiltrazione efficace in un bacino dell'Italia centrale: confronto con analoghi bacini rappresentativi di diversa litologia, *Geologia Applicata e Idrogeologia*, 17, 437–452, 1982.

Brancaccio, L., Cinque, A., and Sgrosso, I.: L'analisi dei versanti di faglia come strumento per la ricostruzione di eventi neotettonici, *Memorie Società Geologica Italiana*, 19, 621–626, 1978.

Brusdon, C., Mc Clatchey, J., and Unwin, D. J.: Spatial variations in the average rainfall–altitude relationship in Great Britain: an approach using geographically weighted regression, *Int. J. Climatol.*, 21, 455–466, 2001.

Burdon, D. J.: Hydrogeology of some karstic areas of Greece. *Actes de Colloque de Dubrovnik sur l'Hydrologie des roches calcaires fessures*, A.I.H.S.-UNESCO, 73, 308–317, 1965.

Estimating annual effective infiltration coefficient

V. Allocca et al.

[Title Page](#)

[Abstract](#)

[Introduction](#)

[Conclusions](#)

[References](#)

[Tables](#)

[Figures](#)

[◀](#)

[▶](#)

[◀](#)

[▶](#)

[Back](#)

[Close](#)

[Full Screen / Esc](#)

[Printer-friendly Version](#)

[Interactive Discussion](#)



Estimating annual effective infiltration coefficient

V. Allocata et al.

[Title Page](#)[Abstract](#)[Introduction](#)[Conclusions](#)[References](#)[Tables](#)[Figures](#)[|◀](#)[▶|](#)[◀](#)[▶](#)[Back](#)[Close](#)[Full Screen / Esc](#)[Printer-friendly Version](#)[Interactive Discussion](#)

Bull, W. B.: Tectonic geomorphology of mountains, a new approach to paleoseismology, Blackwell Publishing, 316 pp., 2007.

Carroll, R. J. and Ruppert, D.: Transformation and Weighting in Regression, Chapman and Hall, New York, 1988.

5 Celico, P.: Idrogeologia dei massicci carbonatici, delle piane quaternarie e delle aree vulcaniche dell'Italia centromeridionale (Marche e Lazio meridionale, Abruzzo, Molise e Campania), Quaderni della Cassa per il Mezzogiorno, 4, 1–203, 1983.

10 Celico, F., Petrella, P., and Celico, P.: Hydrogeological behaviour of some fault zones in a carbonate aquifer of Southern Italy: an experimentally based model, *Terra Nova*, 18, 308–313, 2006.

Celico, F., Naclerio, G., Bucci, A., Nerone, V., Capuano, P., Carcione, M., Allocata, V., and Celico, P.: Influence of pyroclastic soil on epikarst formation: a test study in southern Italy, *Terra Nova*, 22, 110–115, 2010.

15 Civita, M., Olivero, G., Manzone, L., and Vigna, B.: Approcci sinergici nelle ricerche sui sistemi idrogeologici carbonatici del Piemonte meridionale, *Atti Conv. Ricerca e Protezione delle Risorse Idriche Sotterranee delle Aree Montuose*, 1, 53–86, 1992.

Darcy, H.: *Les Fontaines Publiques de la Ville de Dijon*, Victor Dalmont, Paris, 1–647, 1856.

Del Giudice, G., Padulano, R., and Rasulo, G.: Factors affecting the runoff coefficient, *Hydrol. Earth Syst. Sci. Discuss.*, 9, 4919–4941, doi:10.5194/hessd-9-4919-2012, 2012.

20 De Vita, P., Agrello, D., and Ambrosino, F.: Landslide susceptibility assessment in ash-fall pyroclastic deposits surrounding Somma–Vesuvius: application of geophysical surveys for soil thickness mapping, *J. Appl. Geophys.*, 59, 126–139, 2006.

De Vita, P., Allocata, V., Manna, F., and Fabbrocino, S.: Coupled decadal variability of the North Atlantic Oscillation, regional rainfall and karst spring discharges in the Campania region (southern Italy), *Hydrol. Earth Syst. Sci.*, 16, 1389–1399, doi:10.5194/hess-16-1389-2012, 2012a.

25 De Vita, P., Napolitano, E., Godt, J. W., and Baum, R. L.: Deterministic estimation of hydrological thresholds for shallow landslide initiation and slope stability models: case study from the Somma–Vesuvius area of southern Italy, *Landslides*, online first, doi:10.1007/s10346-012-0348-2, 2012b.

30 Dripps, W. R. and Bradbury, K. R.: The spatial and temporal variability of groundwater recharge in a forested basin in northern Wisconsin, *Hydrol. Process.*, 24, 383–392, 2010.

Drogue, C.: Coefficient d'infiltration ou infiltration efficace, sur le roches calcaires, *Actes du Colloque d'Hydrologie en Pays Calcaire*, Besançon, 15, 121–130, 1971.

Drogue, C.: *Hydrodynamiques of karstic aquifers: experimental sites in the Mediterranea karst, Southern France*, *Inter. Contr. to Hydrogeol. I.A.H.*, 13, 133–149, 1992.

5 European Commission: Directive 2000/60/EC of the European Parliament and of the Council of 23 October 2000 establishing a framework for community action in the field of water policy, *Official Journal L327* of 22 December, 2000.

Fiorillo, F.: Tank-reservoir drainage as a simulation of the recession limb of karst spring hydrographs, *Hydrogeol. J.*, 19, 1009–1019, 2011.

10 Geiger, R.: *Landolt-Börnstein – Zahlenwerte und Funktionen aus Physik, Chemie, Astronomie, Geophysik und Technik*, alte Serie Vol. 3, Ch. Klassifikation der Klimate nach W. Köppen, Springer, Berlin, 603–607, 1954.

Goldscheider, N.: A holistic approach to groundwater protection and ecosystem services in karst terrains, *AQUA mundi*, Am06046, 117–124, 2012.

15 Goldscheider, N. and Drew, D.: Methods, in: *Karst Hydrogeology*, Taylor & Francis, London, 1–264, 2007.

Goovaerts, P.: Geostatistical approaches for incorporating elevation into the spatial interpolation of rainfall, *J. Hydrol.*, 228, 113–129, 2000.

Henderson-Sellers, A. and Robinson, P. J.: *Contemporary Climatology*, John Wiley & Sons, 20 New York, 1986.

Horvat, B. and Rubinic, J.: Annual runoff estimation – an example of karstic aquifers in the transboundary region of Croatia and Slovenia, *Hydrolog. Sci. J.*, 51, 314–324, 2006.

Houze, R. A.: Orographic effects on precipitating clouds, *Rev. Geophys.*, 50, 1–47, 2012.

Kessler, H.: Water balance investigation in the karstic region of Hungary, *Actes de Colloque de Dubrovnik sur l'Hydrologie des roches calcaires fessures*, A.I.H.S.-UNESCO, 73, 91–105, 25 1965.

Kiraly, L.: Rapport sur l'état actuel des connaissances dans le domaines des caractères physiques des roches karstiques, edited by: Burger, A. and Dubertret, L., *Hydrogeology of Karstic Terrains*, Int. Union of Geol. Sciences, B, 3, 53–67, 1975.

30 Kiraly, L.: Karstification and Groundwater Flow, in: "Evolution of Karst: From Prekarst to Cessation", edited by: Gabrovsek, F., Zalozba ZRC, Postojna-Ljubljana, 155–190, 2002.

Estimating annual effective infiltration coefficient

V. Allocca et al.

[Title Page](#)

[Abstract](#)

[Introduction](#)

[Conclusions](#)

[References](#)

[Tables](#)

[Figures](#)

[◀](#)

[▶](#)

[◀](#)

[▶](#)

[Back](#)

[Close](#)

[Full Screen / Esc](#)

[Printer-friendly Version](#)

[Interactive Discussion](#)



Klimchouk, A. B.: The formation of Epikarst and its role in Vadose Speleogenesis, edited by: Klimchouk, A. B., Ford, D. C. Palmer, A. N., and Dreybrodt, W., *Speleogenesis, Evolution of Karst Aquifers*, Huntsville, Nat. Speleol. Soc., 91–99, 2000.

Mangin, A.: Contribution à l'étude hydrodynamique des aquifères karstiques, *Ann Spéléol*, 29, 5 283–332, 1975a.

Mangin, A.: Contribution à l'étude hydrodynamique des aquifères karstiques, *Ann Spéléol*, 29, 495–601, 1975b.

Mangin, A.: Contribution à l'étude hydrodynamique des aquifères karstiques, *Ann Spéléol*, 30, 21–124, 1975c.

10 Marquínez, J., Lastra, J., and García, P.: Estimation models for precipitation in mountainous regions: the use of GIS and multivariate analysis, *J. Hydrol.*, 270, 1–11, 2003.

Naclerio, G., Petrella, E., Nerone, V., Allocca, V., De Vita, P., and Celico, F.: Influence of top-soil of pyroclastic origin on microbial contamination of groundwater in fractured carbonate aquifers, *Hydrogeol. J.*, 16, 1057–1064, 2008.

15 Naclerio, G., Nerone, V., Bucci, A., Allocca, V., and Celico, F.: Role of organic matter and clay fraction on migration of *Escherichia Coli* cells through pyroclastic soils, southern Italy, *Colloid. Surface. B*, 72, 57–61, 2009.

Patacca, E. and Scandone, P.: Geology of the Southern Apennines, *Italian Journal of Geosciences*, 7, 75–119, 2007.

20 Roe, G. H.: Orographic precipitation, *Annual Rev. Earth Pl. Sc.*, 33, 645–671, 2005.

Santoro, M.: Sulla applicabilità della formula di Turc per il calcolo della evapotraspirazione effettiva in Sicilia, in: *Proceedings I International Conference on Groundwater*, I. A. H., Palermo, 1970.

25 Scanlon, B. R., Healy, R. W., and Cook, P. G.: Choosing appropriate techniques for quantifying groundwater recharge, *Hydrogeol. J.*, 10, 18–39, 2002.

Sodeman, P. C. and Tysinger, J. E.: Effect of forest cover upon hydrologic characteristics of a small watershed in limestone region of East Tennessee, *Actes de Colloque de Dubrovnik sur l'Hydrologie des roches calcaires fessures*, A.I.H.S.-UNESCO, 73, 135–151, 1965.

30 Soulios, G.: Infiltration efficace dans le karst hellénique, *J. Hydrol.*, 75, 343–356, 1984.

Turc, L.: Le bilan d'eau des sols. Relation entre les précipitations, l'évaporation et l'écoulement, *Ann. Agron.*, 5, 491–595, 1954.

Estimating annual effective infiltration coefficient

V. Allocca et al.

[Title Page](#)[Abstract](#)[Introduction](#)[Conclusions](#)[References](#)[Tables](#)[Figures](#)[◀](#)[▶](#)[◀](#)[▶](#)[Back](#)[Close](#)[Full Screen / Esc](#)[Printer-friendly Version](#)[Interactive Discussion](#)

Estimating annual effective infiltration coefficient

V. Allocca et al.

[Title Page](#)[Abstract](#)[Introduction](#)[Conclusions](#)[References](#)[Tables](#)[Figures](#)[|◀](#)[▶|](#)[◀](#)[▶|](#)[Back](#)[Close](#)[Full Screen / Esc](#)[Printer-friendly Version](#)[Interactive Discussion](#)

Vilimonovic, J.: A contribution of the study of groundwater intake recharge in karst, *Actes de Colloque de Dubrovnik sur l'Hydrologie des roches calcaires fessures*, A.I.H.S.-UNESCO, 73, 482–499, 1965.

Vuglinski, V. S.: Methods for the study of laws for the distribution of precipitation in mediu-high mountains (illustrated by the Vitim River Basin), *Distribution of precipitation in Mountainous Areas*, WMO Pub., 326, 212–221, 1972.

White, W. B.: Conceptual models for carbonate aquifer, *Ground Water*, 7, 15–21, 1969.

White, W. B.: Karst hydrology: recent developments and open questions, *Eng. Geol.*, 65, 85–105, 2002.

Estimating annual effective infiltration coefficient

V. Allocata et al.

Table 1. AEIC and mean AEIC_S estimation for the investigated sample karst aquifers. Values are related to the mean value of the AEP linear regression models with altitude.

ID	Karst aquifer	Area (km ²)	Summit flat/endorheic area (%)	V_{outflow} (10 ⁶ m ³)	V_{inflow} (10 ⁶ m ³)	AEIC (%)	AEIC _S (%)	ARC (%)
17a	Matese (a)	120	34	95.2	138.1	69	52	48
27	Terminio	167	43	169.7	213.3	79	64	36
31a	Accellica (a)	35	0	18.3	36.9	50	50	50
32	Cervialto	129	20	126.1	178.4	71	63	37

- [Title Page](#)
- [Abstract](#) [Introduction](#)
- [Conclusions](#) [References](#)
- [Tables](#) [Figures](#)
- [◀](#) [▶](#)
- [◀](#) [▶](#)
- [Back](#) [Close](#)
- [Full Screen / Esc](#)
- [Printer-friendly Version](#)
- [Interactive Discussion](#)



Estimating annual effective infiltration coefficient

V. Allocata et al.

Table 2. Data and estimations of AEIC, AEIC_s, ARC and mean annual groundwater recharge for karst aquifers of the study area. In the last column, the mean annual groundwater outflow, estimated for some of the karst aquifers by other hydrogeological studies (Celico, 1983; Allocata et al., 2007) are reported; values estimated in this study for the four sample karst aquifers (ID 17a, 27, 31a and 32) are reported.

ID	Karst aquifer	Area (km ²)	AEP (10 ⁶ m ³)	Limestone area (%)	Summit flat and endorheic area (%)	AEIC (%)	AEIC _s (%)	ARC (%)	Mean annual groundwater recharge (10 ⁶ m ³)	Mean annual groundwater outflow (10 ³ m ³)
1	Cerella	137	101.1	100	0	56	56	44	56.6	–
2	Simbruini	1075	963.2	94	12	62	57	43	597.2	–
3	Cornacchia	723	679.6	90	7	59	56	44	401.0	–
4	Marsicano	204	172.4	94	5	58	56	44	100.0	–
5	Genzana	277	225.5	10	34	66	49	51	148.8	–
6	Rotella	40	32.0	100	40	77	62	38	24.6	–
7	Porrara	63	47.4	100	25	69	59	41	32.7	–
8	Lepini	483	478.2	100	2	57	57	43	272.6	400.5
9	Colli Campanari	88	61.8	0	12	54	48	52	33.4	–
10	Capraro	70	41.0	0	5	51	48	52	20.9	–
11	Campo	16	11.1	0	13	55	48	52	6.1	–
12	Circeo	6	3.3	0	0	48	48	52	1.6	–
13	Ausoni	822	686.4	99	15	64	58	42	439.3	507.7
14	Venafro	362	288.2	74	11	60	55	45	172.9	269.3
15	Totila	183	97.9	0	8	52	48	52	50.9	–
16	Maio	93	65.7	98	12	63	58	42	41.4	–
17	Matese	480	552.5	65	15	61	55	39	303.8	375
17a	Matese (a)	120	138.1	97	34	74	60	26	102.2	95.2
18	Tre confini	28	23.2	0	4	50	48	52	11.6	–
19	Moschiaturo	85	75.4	0	7	51	48	52	38.5	–
20	Massico	29	20.3	89	0	55	55	45	11.2	–

Estimating annual effective infiltration coefficient

V. Allocata et al.

Table 2. Continued.

ID	Karst aquifer	Area (km ²)	AEP (10 ⁶ m ³)	Limestone area (%)	Summit flat and endorheic area (%)	AEIC (%)	AEIC _S (%)	ARC (%)	Mean annual groundwater recharge (10 ⁶ m ³)	Mean annual groundwater outflow (10 ⁶ m ³)
21	Maggiore	157	112.9	99	0	56	56	44	63.2	56.7
22	Camposauro	50	46.8	99	4	58	56	44	27.1	–
23	Tifatini	80	51.7	90	2	56	56	44	28.9	25.2
24	Taburno	43	52.1	81	4	57	55	45	29.7	–
25	Durazzano	52	40.3	100	0	56	56	44	22.6	–
26	Avella	334	328.3	100	9	61	57	43	200.3	–
27	Terminio	167	213.3	100	43	78	62	38	166.3	169.7
28	Capri	9	5.1	93	0	56	56	44	2.8	–
29	Lattari	244	211.8	75	0	54	54	46	114.4	–
30	Salerno	46	33.8	13	0	49	49	51	16.5	21.1
31	Accellica	171	180.4	33	0	51	51	49	92.0	107.6
31a	Accellica (a)	35	36.9	32	0	51	51	49	18.8	18.3
32	Cervialto	129	178.4	98	20	67	58	42	119.5	126.1
33	Polveracchio	117	147.1	81	0	55	55	45	80.9	103.1
34	Marzano	292	226.6	97	13	63	57	43	142.8	–
35	Alburni	254	295.1	99	42	78	62	38	230.2	233.4
36	Cervati	318	389.6	81	13	62	56	44	241.5	220.8
37	Motola	52	61.3	100	4	59	57	43	36.2	37.8
38	Maddalena	307	263.7	59	21	64	54	46	168.8	97.8
39	Forcella	217	209.4	86	5	58	56	44	121.5	–
40	Bulgheria	100	78.5	68	1	54	54	46	42.4	42.5

Discussion Paper | Estimating annual effective infiltration coefficient

V. Allocata et al.

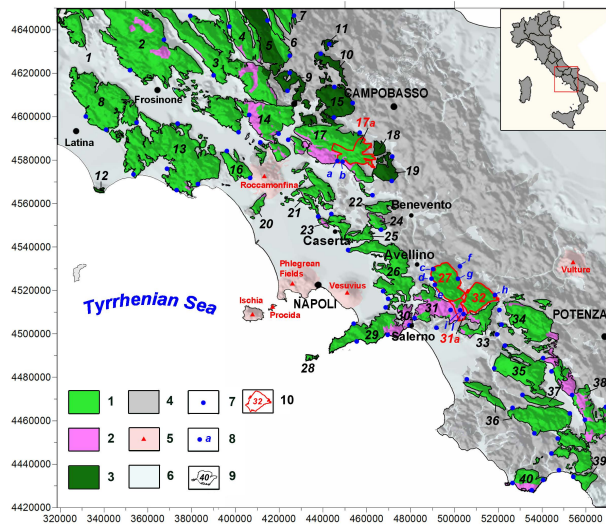


Fig. 1. Map of the karst aquifers of the southern Apennines. Key to symbols: (1) Limestone and dolomitic limestone units of the carbonate platform series (Jurassic-Paleogene); (2) Dolomitic units of the carbonate platform series (Triassic-Liassic); (3) Calcareous-marly units of the outer basin series (Triassic-Paleogene); (4) Pre-, syn- and late- orogenic molasses and terrigenous units (Cretaceous-Pliocene); (5) Volcanic centres (Pliocene-Quaternary); (6) Alluvial and epiclastic units (Quaternary); (7) Main basal springs of karst aquifers; (8) Basal karst springs considered in the hydrological budget (a and b: Maretto and Torano; c: Salza Irpina; d and e: Serino; f: Baiardo; g: Cassano Irpino; h: Sanità; i: Avella; l: Ausino-Ausinetto); (9) Hydrogeological boundary and identification number of the karst aquifers; (10) Hydrogeological boundary and identification number of the karst aquifers considered for the hydrological budget (where present the boundary of the groundwater sub-basin is indicated by a dashed line).

Estimating annual effective infiltration coefficient

V. Allocca et al.

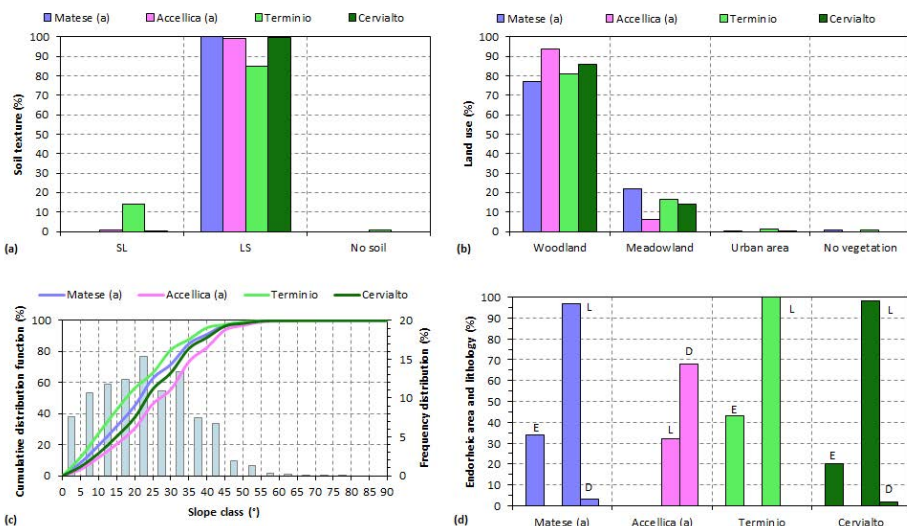


Fig. 2. Soil texture type, land use and geomorphological characteristics of the four sample karst aquifers. **(a)** Soil texture frequency (SL Sandy Loam, LS Loamy Sand). **(b)** Land use frequency. **(c)** Slope of karst aquifers frequency. **(d)** Summit endorheic and flat areas frequency (E) and lithology (L = limestone; D = dolomite).

Estimating annual effective infiltration coefficient

V. Allocata et al.

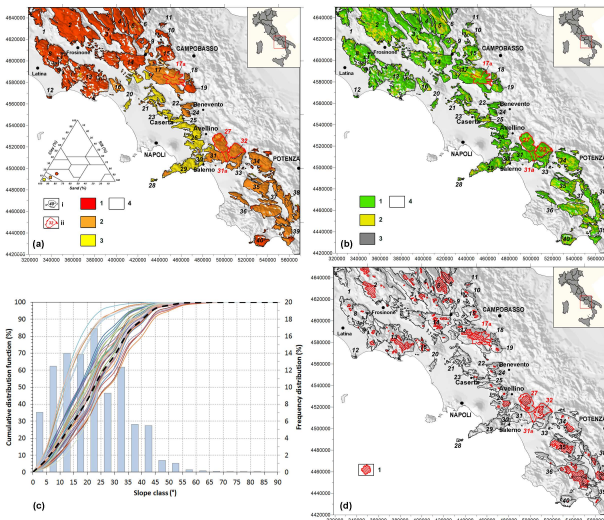


Fig. 3. **(a)** Soil texture map. Common symbols: (i) Hydrogeological boundary and identification number of the karst aquifers; (ii) Hydrogeological boundary and identification number of the sample karst aquifers; dashed line indicates the boundary of the groundwater basin. Key to symbols: (1) Sandy Loam soil; (2) Loamy Sand soil; (3) Sandy soil; (4) Area with no soil. **(b)** Land use map. Key to symbols: (1) Woodland; (2) Meadowland; (3) Urban Area; (4) No vegetation area. **(c)** Frequency analysis of the slope angle distribution for the karst aquifers. Key to symbol: (colored line) Cumulative distribution of single karst aquifer; dashed black line) Mean cumulative distribution; histogram) Mean frequency distribution. **(d)** Summit flat areas and endorheic watersheds map. Key to symbol: (1) Limits of endorheic watershed.

[Title Page](#)

[Abstract](#)

[Introduction](#)

[Conclusions](#)

[References](#)

[Tables](#)

[Figures](#)

[◀](#)

[▶](#)

[◀](#)

[▶](#)

[Back](#)

[Close](#)

[Full Screen / Esc](#)

[Printer-friendly Version](#)

[Interactive Discussion](#)

Estimating annual effective infiltration coefficient

V. Allocca et al.

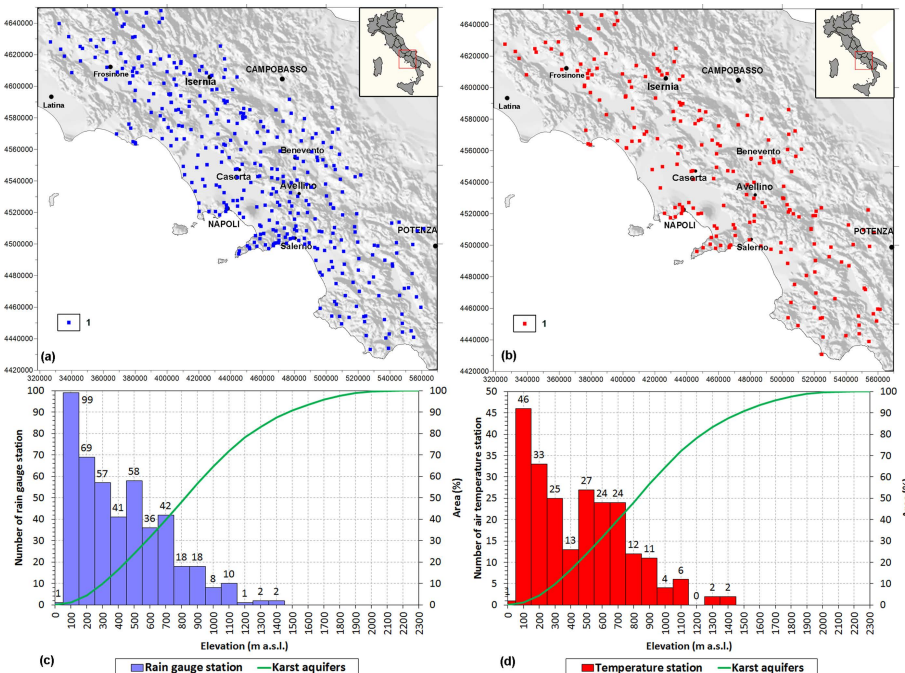


Fig. 4. Areal distributions of rain gauge stations (a) and air temperature stations (b). Comparisons between the altitudinal distribution of rain gauge stations (c), air temperature stations (d) and hypsometric curve of the 40 karst aquifers in the study area.

Estimating annual effective infiltration coefficient

V. Allocata et al.

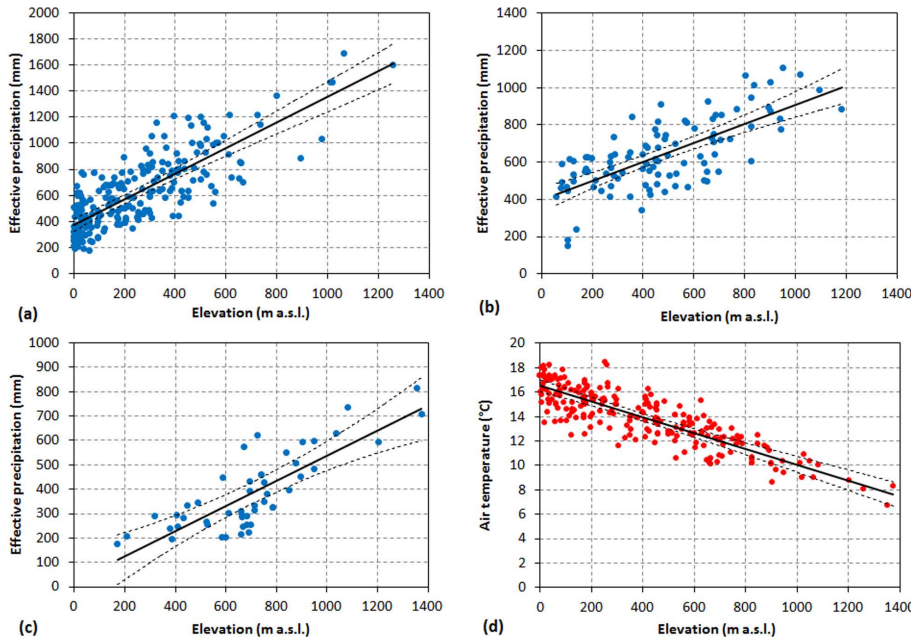


Fig. 5. Linear correlations and confidence limits (95 %) between mean annual effective precipitation (AEP) and altitude for upwind zone **(a)**, first downwind zone **(b)** and second downwind zone **(c)**. The correlation between mean annual air temperature and altitude is also shown **(d)**.

- [Title Page](#)
- [Abstract](#) [Introduction](#)
- [Conclusions](#) [References](#)
- [Tables](#) [Figures](#)
- [◀](#) [▶](#)
- [◀](#) [▶](#)
- [Back](#) [Close](#)
- [Full Screen / Esc](#)
- [Printer-friendly Version](#)
- [Interactive Discussion](#)

Estimating annual effective infiltration coefficient

V. Allocata et al.

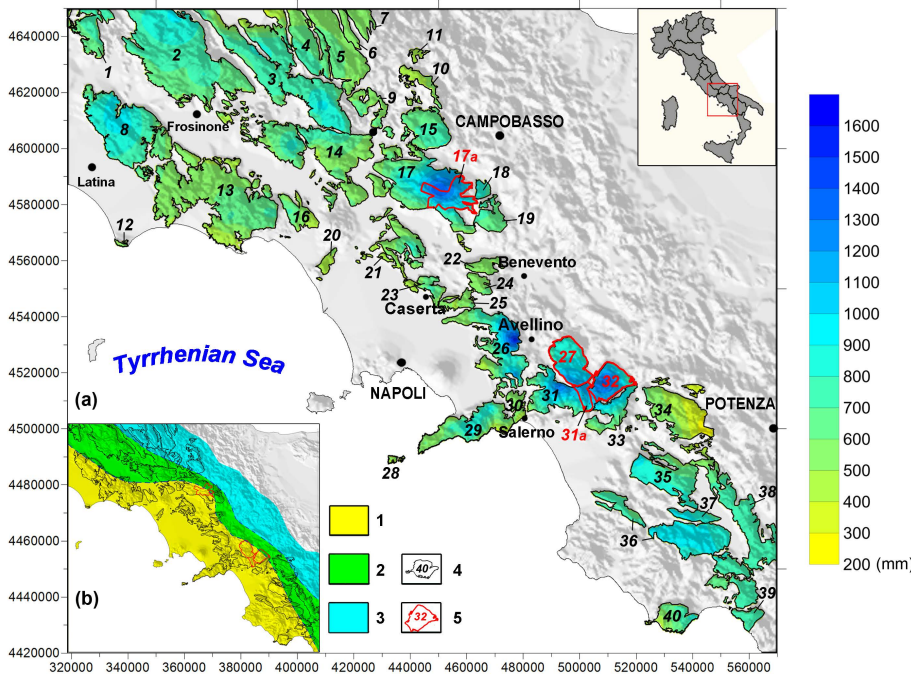


Fig. 6. Distributed models of annual effective precipitation (AEP) based on homogeneous zones (a). Key to symbol: (1) Upwind zone; (2) First downwind zone; (3) Second downwind zone; (4) Hydrogeological boundaries and identification number of the karst aquifers; (5) Hydrogeological boundaries and identification number of the karst aquifers considered for the hydrological budget.

- [Title Page](#)
- [Abstract](#) [Introduction](#)
- [Conclusions](#) [References](#)
- [Tables](#) [Figures](#)
- [◀](#) [▶](#)
- [◀](#) [▶](#)
- [Back](#) [Close](#)
- [Full Screen / Esc](#)
- [Printer-friendly Version](#)
- [Interactive Discussion](#)

Estimating annual effective infiltration coefficient

V. Allocata et al.

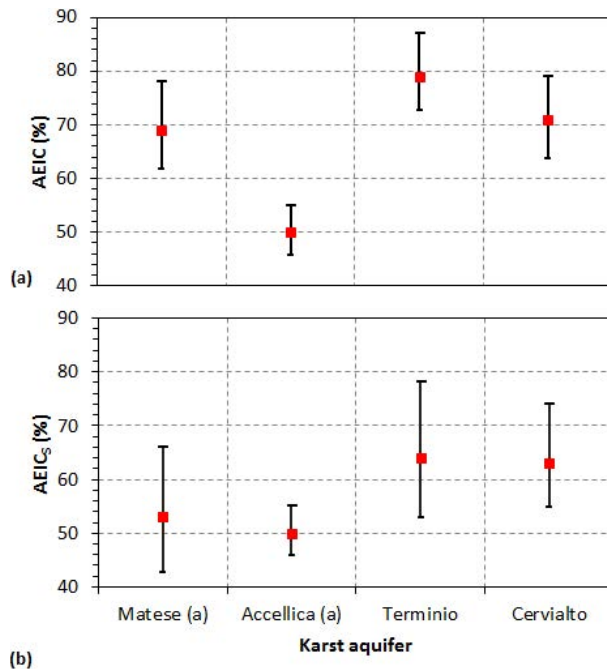


Fig. 7. AEIC (a) and AEIC_S (b) estimations for the four sample karst aquifers obtained considering uncertainties of the annual effective precipitation and air temperature regression models (95 % confidence limits).

Estimating annual effective infiltration coefficient

V. Allocata et al.

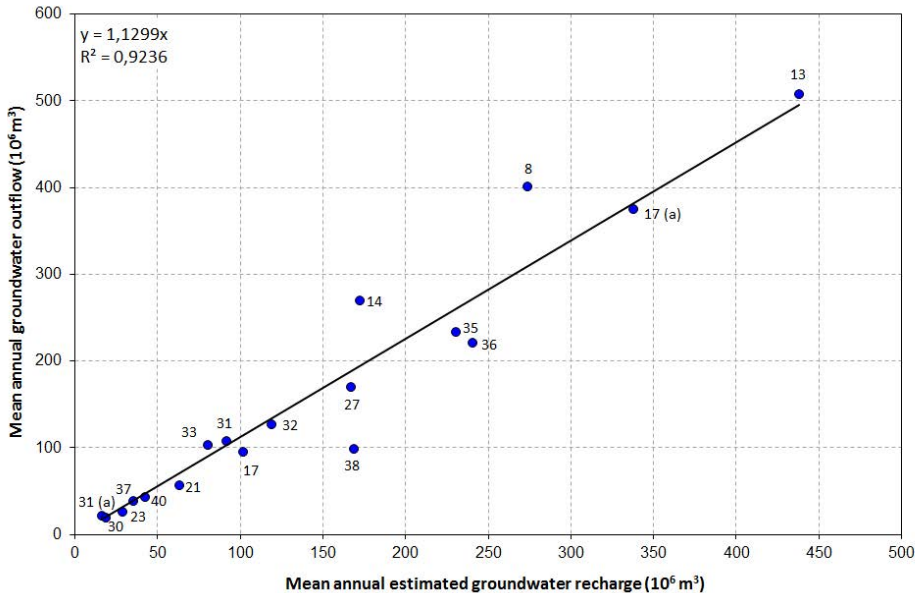


Fig. 8. Correlation between mean annual groundwater outflow assessed by non-systematic spring discharges measurements and mean annual estimated groundwater recharge. The numbers correspond to the ID of the aquifers.